PHYSICAL REVIEW B VOLUME 17, NUMBER 2 15 JANUARY 1978

Resonant Raman effect of O_3^- in γ-irradiated $Ba(ClO_3)_2H_2O$ and $AgClO_3$

G. M. Gualberto, M. A. Tenan, H. Vargas, and L. C. M. Miranda
Instituto de Física, Universidade Estadual de Campinas, 13100 Campinas, São Paulo, Brazil

J. Pelzl
Institut für Experimentalphysik VI, Ruhr-Universität, 463-Bochun, West Germany

(Received 7 March 1977)

Resonant vibrational Raman measurements of O_3^- in γ-irradiated $Ba(ClO_3)_2H_2O$ and $AgClO_3$ are reported. It is concluded that the O_3^- ions occupy two nonequivalent sites in the lattice. A simple model describing the unusual relative Raman intensities is also presented.

For some time, resonant Raman spectroscopy has been proved to be an effective tool in the investigation of defects in solids.[1-4] The object of the present paper is to report on the vibrational resonant Raman (RR) effect of O_3^- centers in γ-irradiated $Ba(ClO_3)_2H_2O$ and $AgClO_3$. The observation of trapped paramagnetic centers in γ-irradiated single crystals of many different sulphates, chlorates, and nitrates has already been reported in several papers using ESR studies[5-11] as well as Raman studies.[12,13] Due to the multiple site occupancy and orientation of these centers in the lattice, their identification via paramagnetic resonance was not too obvious at the beginning. The paramagnetic-resonance data on γ-irradiated alkali-metal chlorates tell us that the radicals formed by this ionizing radiation seem all to behave as oriented free charges (*g* value of about 2.0).[5-13] This means that these irradiated systems provide us a unique possibility for studying isolated oriented radicals. We report in this article on vibrational resonant Raman (RR) measurements of O_3^- centers in γ-irradiated $Ba(ClO_3)_2H_2O$ and $AgClO_3$. Resonance Raman scattering was first used to determine multiple site occupancy of O_3^- ions in single crystals of $KClO_3$ and $NaClO_3$ in Ref. 13. As is shown in the following the Raman effect proved indeed to be an effective tool for investigating the multiple-site occupancy and orientations of the O_3^- centers. Furthermore the relative vibrational Raman intensities exhibited a strictly unusual behavior which is associated with the small differences in the static field felt by O_3^- in the nonequivalent sites occupied by them.

The O_3^- centers (concentration of about 10^{16} cm^{-3}) were obtained after 10 Mrad of γ irradiation at room temperature from a ^{60}Co source. The ESR spectra of irradiated single crystals of $Ba(ClO_3)_2H_2O$ and $AgClO_3$ provided us with the number of crystallographically nonequivalent O_3^- ions and their orientations in the $Ba(ClO_3)_2H_2O$ and $AgClO_3$ lattices as discussed in Refs. 11 and 12. It was concluded then that the O_3^- ions occupy two nonequivalent sites in the crystal. The same conclusions are also reached from the resonant Raman results. The resonant Raman experiments in $Ba(ClO_3)_2H_2O$ were performed in backscattering configuration with the 4579-Å Ar line at room temperature from samples having natural faces. In the case of $AgClO_3$ the Raman spectrum was recorded at 4.2 °K also in backscattering configuration with the 5145-Å Ar line. The optical-absorption and resonant Raman data of ν_1 (the symmetric stretching mode of O_3^-) and its overtones are presented in Tables I and II. Both the ground and excited vibronic bands assigned to progressions of the symmetric stretching mode ν_1 and ν_1' in the ground and excited states, respectively, were

TABLE I. Frequencies ν (cm^{-1}) and intensities I of electronic absorption bands and Raman lines of O_3^- in γ-irradiated $Ba(ClO_3)_2H_2O$.

	Raman lines $x(zz)\bar{x}$			
Transition	ν_1^a	I_a	ν_1^b	I_b
0-1	1036	7.8	1045	2.8
0-2	2062	4.9	2074	4.0
0-3	3050	2.6	3064	2.5
0-4	4024	1.4	4041	2.0
$\omega_0'=1006$ cm^{-1}	$\omega_0^a=1050$ cm^{-1}		$\omega_0^b=1060$ cm^{-1}	
$\omega_0'X_0=7.8$ cm^{-1}	$(\omega_0X_0)^a=11.2$ cm^{-1}		$(\omega_0X_0)^b=12.6$ cm^{-1}	

TABLE II. Frequencies ν (cm^{-1}) and intensities I of electronic absorption bands and Raman lines of O_3^- in γ-irradiated $AgClO_3$.

	Raman lines $x(zz)\bar{x}$			
Transition	ν_1^a	I_a	ν_1^b	I_b
0-1	1004	9.0		
0-2	1995	3.0	2012	0.4
0-3	2981	1.7	2992	1.3
0-4	3949	0.7	3956	0.5
$\omega_0'=1028$ cm^{-1}	$\omega_0^a=1009$ cm^{-1}		$\omega_0^b=1023$ cm^{-1}	
$\omega_0'X_0'=18$ cm^{-1}	$(\omega_0X_0)^a=5.4$ cm^{-1}		$(\omega_0X_0)^b=8.4$ cm^{-1}	

determined from the simple diatomic term value expression[14]

$$\nu_1(\eta) = \omega_0\eta - (\omega_0 X_0)\eta^2 . \qquad (1)$$

The prime in Tables I and II denotes excited-state properties. Fig. 1 shows the resonant Raman spectrum of O_3^- in $Ba(ClO_3)_2H_2O$ recorded in the $x(zz)\bar{x}$ configuration where x and z are parallel to the [110] and [001*] directions, respectively. This spectrum clearly shows a splitting of the $\eta\nu_1$ (A_g) bands of O_3^- into two components ν_1^a and ν_1^b. Graphs of the relative intensities as a function of the vibrational quantum number are shown in Fig. 2. The relative intensities were measured using the ν_1 (A_g) mode of ClO_3^- as reference[13] corrected for instrument response. Figures 3 and 4 present the corresponding Raman results for $AlClO_3$ recorded in the $x(zz)\bar{x}$ configuration where x and z are parallel to the [110] and [001] directions, respectively. Again, the $\eta\nu_1$ bands of O_3^- in $AgClO_3$ exhibits a splitting into two components. The splitting of ν_1 and its overtones into two components suggests that the O_3^- ions produced by radiolysis of ClO_3^- are trapped at two crystallographically distinct sites, possibly those formerly occupied by the ClO_3^- precursors. This is further supported by the ESR measurements.[10-12] The observed doublet splitting of the $\eta\nu_1$ mode are therefore resultant from different orientations of O_3^- ions at these sites (orientational splitting). The magnitude of this splitting between the pair of components is a measure of the difference in the static field for two nonequivalent orientations of O_3^- ions at these sites. Referring to Tables I and II and Figs. 2 and 4 one notes that the orientational effects which are caused by the anisotropy of the static field at the two sites are reflected not only in the splitting between components, and thus between the ω_0 values, but also in the small differences between the values of $\omega_0 X_0$.

The kind of behavior depicted in Figs. 2 and 4 for the relative Raman intensities may be understood if one assumes a simple model involving a simple intermediate state and electron-phonon interaction with a single phonon mode similar to that developed in Ref. 15. The Raman cross section for light scattered from $\vec{k}_i$ to $\vec{k}_s$ can be written as $\sigma = (e^4\omega_s/m^4c^4\omega_i)\,|M|^2$, where

$$M = \sum_e \left(\frac{\langle f|\vec{\epsilon}_s\cdot\vec{p}|e\rangle\langle e|\vec{\epsilon}_i\cdot\vec{p}|i\rangle}{E_e - E_i - \hbar\omega_L} + \frac{\langle f|\vec{\epsilon}_i\cdot\vec{p}|e\rangle\langle e|\vec{\epsilon}_s\cdot\vec{p}|i\rangle}{E_e - E_i + \hbar\omega_s} \right). \qquad (2)$$

Here we assume that the states are separated into an electronic and a vibrational part (Frank-Condon approximation) and that the matrix elements of $\vec{p}$ are independent of the vibrational coordinates. The latter then enter M only as overlap integrals. Now, if the exciting frequency ω_L is near resonance, the first term in Eq. (2) is much the larger and we can neglect the second term. Furthermore, we assume that only one intermediate electronic state is important. With these assumptions, a

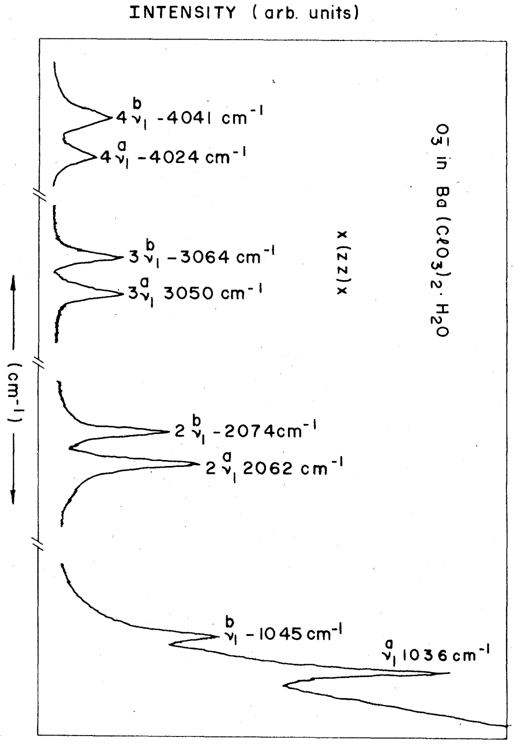

FIG. 1. Resonant Raman spectrum of O_3^- in $Ba(ClO_3)_2H_2O$. The laser frequency is the 4579-Å Ar line.

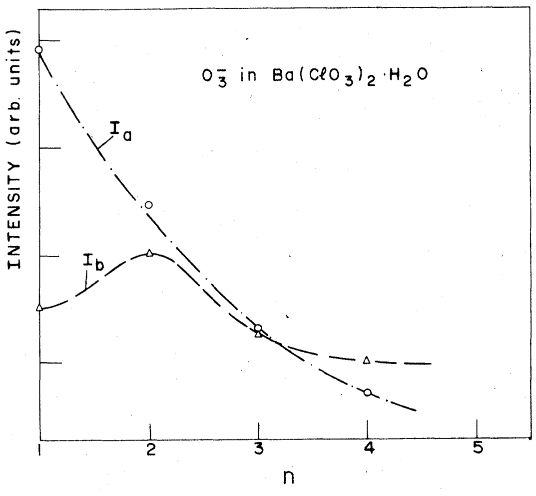

FIG. 2. Relative Raman intensities of O_3^- in $Ba(ClO_3)_2H_2O$ as a function of the vibrational quantum n.

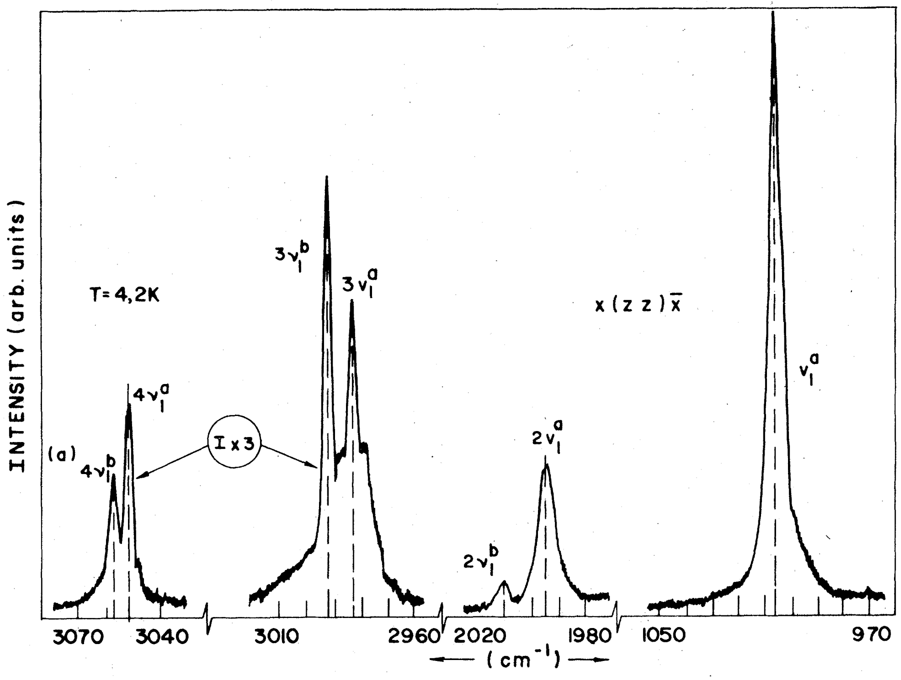

FIG. 3. Resonant Raman spectrum of O_3^- in $AgClO_3$. The exciting laser frequency is the 5145-Å Ar line.

process creating n-vibrational quanta has the form

$$M=\langle f|\vec{\epsilon}_s\cdot\vec{p}\,|e\rangle\,\langle e|\vec{\epsilon}_i\cdot\vec{p}\,|i\rangle S_n/\hbar\omega_0' \,, \tag{3}$$

where $\hbar\omega_0'$ is the vibrational quantum in the upper electronic state and S_n takes the simple form

$$S_n=\sum_{n_e}\frac{\langle 0|n_e\rangle\,\langle n_e|n\rangle}{n_e+\lambda}\,. \tag{4}$$

In arriving at Eq. (4) we have written the energy denominator in units of $\hbar\omega_0'$. Here λ defines the photon matching of the resonance, i.e., $\lambda=(E_e-E_0-\hbar\omega_L)/\hbar\omega_0'$. The sum in Eq. (4) is over all states n_e of the excited oscillator with ω_0'. The initial and final states are of the ground-state oscillator with frequency ω_0. The minimum energy in the upper state is at a coordinate position displaced by r, say, from the ground-state equilibrium position so that the peak absorption takes place with the creation of $X=M\omega_0' r^2/2\hbar$ phonons. The parameter X represents alternatively a measure of the effective strength of the coupling between the electron and the vibrational mode. The general case of $\omega_0'\neq\omega_0$ has been dealt with in Ref. 15. Here we shall consider only the case of $\omega_0'\simeq\omega_0$ which is more appropriate for the present experimental situation (see Tables I and II).

Using the properties of harmonic-oscillator function, we find[15]

$$S_n=\left(\frac{x^n}{n!}\right)^{1/2}\frac{d^nS_0}{dx^n}\,, \tag{5}$$

where

$$S_0=\frac{e^{-x}}{x^\lambda}\int_0^x dt\,e^t t^{\lambda-1}=e^{-x}\Gamma(\lambda)\gamma^*(\lambda,\,-x), \tag{6}$$

$\gamma^*(\lambda,\,-x)$ being the modified incomplete γ function.[16] Taking the derivatives of Eq. (6), S_n can be written in a readily calculable form as

$$S_n=\left(\frac{x^n}{n!}\right)^{1/2}\left(e^{-x}\Gamma(\lambda)\gamma^*(\lambda,\,-x)\sum_{\nu=0}^{n}\binom{n}{\nu}(\lambda)_\nu x^{-\nu}-\sum_{\nu=1}^{n}\binom{n}{\nu}\sum_{\mu=1}^{\nu}(-1)^{\nu-1}(\lambda+\mu)_{\nu-\mu}x^{-(\nu+1-\mu)}\right), \tag{7}$$

where $(a)_\nu=a(a+1)\cdots(a+\nu-1)$ is the Poschhammer's symbol[16] $[(a)_0=1)]$. The variation of S_n with n close to resonance (say, $\lambda=0.1$) is shown in Fig. 5. It follows from Fig. 5 that near resonance and for $x\gg\lambda$ the n-phonon process may become stronger than the $(n-1)$-phonon process whereas, for x and λ of the same order of magnitude, S_n is smaller than S_{n-1}. In other words, depending upon the effective electron-phonon coupling (i.e., the value of x) the resonant vibrational Raman scattering may either present a maximum with respect with n at $n\sim x$ (strong coupling, x

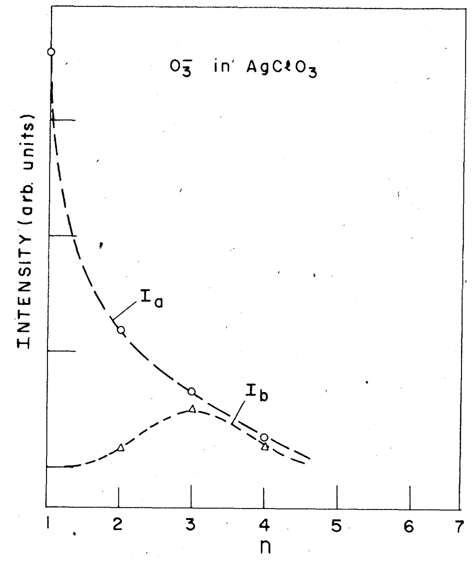

FIG. 4. Relative Raman intensities of O_3^- in AgClO$_3$ as a function of the vibrational quantum number n. Here the symbol $I \times 3$ in the third and fourth harmonics means that the displayed intensity is multiplied by a factor of 3.

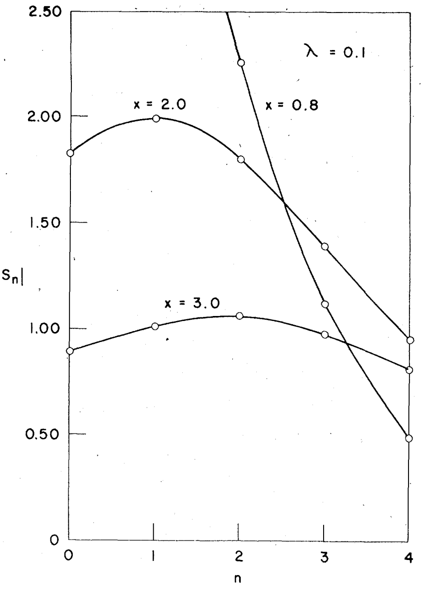

FIG. 5. Variation of the resonant Raman scattering matrix element $|S_n|$ with the vibrational quantum number n.

$\gg \lambda$) or exhibit a normal behavior, namely, always decreasing (weak coupling, $x \sim \lambda$). We believe this simple calculation confirms the hypothesis that the observed splitting of the $n\nu_1$ vibrational Raman lines as being due to O_3^- located at two nonequivalent sites. The component $\nu_1 a$ in Figs. 2 and 4 corresponds to a situation where the O_3^- in one site has a weaker electron-phonon coupling ($x^a \sim \lambda$) than in the case of component ν_1^b at the other site ($x^b \gg \lambda$). This difference in the value of x is of course due to the difference in static field effects at these two sites occupied by O_3^-.

Although this model calculation is sufficiently general the actual observation at resonance of a maximum in $|S_n|$ for $n \sim x$ depends basically on the value of x. In the case of F centers,[17,18] x is typically of the order of 50 which makes it outside the experimental capabilities. Furthermore, it should also be noted from Fig. 5 that near resonance and for $x \gg \lambda$ the electronic Raman intensity, which is proportional to S_0, should be weaker than the first few vibrational overtone intensities. This could possibly be observed in the case of NO (the electronic ground state is a doublet) in γ-irradiated nitrates. This experiment is now in progress in our laboratory.

In conclusion, we would like to acknowledge several useful discussions with Dr. S. P. S. Porto, Dr. C. Rettori, Dr. M. Fóglio, and Dr. J. F. Scott.

---

[1] J. F. Scott, R. C. C. Leite, and T. C. Damen, Phys. Rev. 188, 1285 (1969).

[2] A. Kiel and J. F. Scott, Phys. Rev. B 2, 2033 (1970).

[3] C. K. N. Patel and E. D. Shaw, Phys. Rev. Lett. 24, 451 (1970).

[4] R. M. Martin and T. C. Damen, Phys. Rev. Lett. 26, 86 (1971).

[5] R. S. Eachus, P. R. Edwards, S. Subramanian, and M. C. R. Symons, J. Chem. Soc. A 7, 1704 (1968).

[6] S. Schlik, J. Chem. Phys. 56, 654 (1972).

[7] D. Suryanarayna and J. Sobhanadri, J. Chem. Phys. 61, 2827 (1974).

[8] H. Vargas, C. Dimitropoulos, O. Constantinescu, and D. Dautreppe Radiat. Eff. 18, 9 (1973).

[9] P. W. Atkins and M. C. R. Symons, *The Structure of Inorganic Radicals* (Elsevier, Houston, 1967).

[10] E. C. Silva, G. M. Gualberto, H. Vargas, and C. Rettori, Chem. Phys. Lett. 37, 138 (1976).

[11] E. C. Silva, G. M. Gualberto, C. Rettori, H. Vargas, M. E. Foglio, and G. E. Barberis, J. Chem. Phys. 65, 3461 (1976).

[12] G. M. Gualberto, H. Vargas, C. A. Arguello, and J. Pelzl, in Fifth International Conference on Raman Spectroscopy, Freiburg University, 1976 (unpublished).

[13] J. B. Bates and J. C. Pigs, J. Chem. Phys. 62, 4227 (1975).

[14] See, e.g., G. Herzberg, *Spectra of Diatomic Molecules* (Van Nostrand, New York, 1950), p. 151.

[15] R. J. Elliott and L. C. M. Miranda, in *Third International Conference on Light Scattering in Solids*, edited by M. Balkanski, R. C. C. Leite, and S. P. S. Porto (Flammarion, Paris, 1972), p. 552.

[16] See, e.g., *Handbook of Mathematical Functions*, edited by M. Abramowitz and I. A. Stegun (U.S. GPO, Washington, D.C., 1964), p. 253.

[17] D. A. Kleinman, Phys. Rev. 134, A423 (1964).

[18] J. M. Worlock and S. P. S. Porto, Phys. Rev. Lett. 15, 697 (1965).